Dications of Fluorenylidenes. Relationship between Electrochemical Oxidation Potentials and Antiaromaticity in Diphenyl-Substituted Fluorenyl Cations

Nancy S. Mills,* Michele A. Benish,[1] and Christie Ybarra

Department of Chemistry, Trinity University, 715 Stadium Drive, San Antonio, Texas 78212-7200

Received December 21, 2000

The antiaromaticity of a series of dications of *p*-substituted diphenylmethylidene fluorenes was explored using three criteria attributed to aromaticity/antiaromaticity. The relative stability of the dications (energetic criterion) was measured via the redox potentials obtained by electrochemical oxidation under very fast sweep rates with microelectrodes. Comparison of redox potentials with those of a model system, *p*-substituted tetraphenylethylenes, shows relatively small destabilization of the potentially antiaromatic fluorenylidene dication. However, the amount of destabilization is comparable with the limited electrochemical data available for other antiaromatic systems. Nucleus independent chemical shifts (NICS) were calculated for these dications (magnetic criterion) and indicated their antiaromaticity. A good linear relationship between experimental and calculated (B3LYP/6-31G(d)) ^{1}H and ^{13}C NMR shifts for the three dications, **3c**, **3e**, and **3f**, for which NMR data has been reported, validated the accuracy of the NICS values. Bond length alternation/elongation (structural criterion) was explored via the harmonic oscillator model of aromaticity (HOMA) using the geometries calculated with density functional theory, but there was insufficient variation to evaluate relative antiaromaticity. In addition, the presence of benzannulation appears to restrict bond length alternation to such an extent that the magnitude of the HOMA index is of little use in evaluating the antiaromaticity of many polycyclic hydrocarbons. Both NICS values and redox potentials for formation of the dication in these systems show a strong linear correlation with σ_p^+ values, with the more antiaromatic fluorenylidene dication possessing the more electron-withdrawing substituent. The correlation between NICS values and redox potentials is also good, as might be expected, suggesting a strong relationship between magnetic and energetic characteristics of antiaromaticity. However, magnetic characteristics appear to be a more sensitive probe than energetic characteristics evaluated through redox potentials or structural characteristics evaluated through HOMA calculations.

The theoretical advances that fueled the search for nonbenzenoid aromatic species, such as the cyclopentadienyl anion and tropylium cation, also suggested the nature of antiaromatic species. The criteria by which aromaticity and antiaromaticity are evaluated fall into the following three general categories, energetic, structural, and magnetic.[2,3] The energetic criterion is based on the observation that benzene is thermodynamically more stable than its open-chain analogues; antiaromatic compounds would be thermodynamically less stable. The difficulty in using this criterion lies in selection of the appropriate open-chain analogue. Kinetic stability has also been considered as an indicator of aromaticity, because it is related to a large HOMO−LUMO gap,[4] which is characteristic of benzene. Aromatic compounds have a large HOMO−LUMO gap and are "harder".[5] Assessment of aromaticity based on structural properties returns to the structure of benzene for the definition of those properties. Thus planarity and lack of bond length alternation are the primary descriptors of this property. The harmonic oscillator model of aromaticity (HOMA)[6−8] allows evaluation of the deviation of bond lengths in a species from the optimal bond length of benzene. This model examines two effects that decrease aromaticity, an increase in bond length alternation (geometrical contribution to dearomatization, GEO) and an increase in the mean bond length (the energetic contribution, EN).[9] Magnetic criteria are based on the existence of a ring current that, while experimentally unobservable, can be measured indirectly through the chemical shift of the protons,[10] the magnetic susceptibility exaltation (Λ), and anisotropy,[11−14] as well as evaluated through the calculated nucleus independent chemical shift (NICS, vide supra).[15] While magnetic properties have been proposed

(1) Current address: Department of Experimental Neuro-Oncology, The University of Texas M. D. Anderson Cancer Center, 1515 Holcombe Blvd., Houston, TX 77030.

(2) Minkin, V. I.; Glukhovtsev, M. N.; Simkin, B. Y. *Aromaticity and Antiaromaticity*; John Wiley and Sons: New York, 1994.
(3) Glukhovtsev, M. *J. Chem. Educ.* **1997**, *74*, 132−136.
(4) Zhou, Z. *Int. Rev. Phys. Chem.* **1992**, *11*, 243−261.
(5) Bird, C. W. *Tetrahedron* **1997**, *53*, 3319−24.
(6) Krygowski, T. M.; Cyranski, M. K. *Chem. Rev.* **2001**, *101*, 1385−1419.
(7) Kruszewski, J.; Krygowski, T. M. *Tetrahedron Lett.* **1972**, 3839−42.
(8) Krygowski, T. M. *J. Chem. Inf. Comput. Sci.* **1993**, *33*, 70−8.
(9) Krygowski, T. M.; Cyranski, M. *Tetrahedron* **1996**, *52*, 1713−22.
(10) Elvidge, J. A.; Jackman, L. M. *J. Chem. Soc.* **1961**, 859−866.
(11) Pascal, P. *Ann. Chim. Phys.* **1910**, *19*, 5−70.
(12) Dauben, H. J. J.; Wilson, D. J.; Laity, J. L. *J. Am. Chem. Soc.* **1968**, *90*, 811−813.
(13) Dauben, H. J., Jr.; Wilson, J. D.; Laity, J. L. *Nonbenzenoid Aromatics*; Snyder, J. P., Ed.; Academic Press: New York, 1971; Vol. II, pp 167−206.
(14) Haberditzl, W. *Angew. Chem., Intern. Ed. Eng.* **1966**, *5*, 288−298.
(15) Schleyer, P. v. R.; Maerker, C.; Dransfeld, A.; Jiao, H.; Hommes, N. J. v. E. *J. Am. Chem. Soc.* **1996**, *118*, 6317−6318.

10.1021/jo001776l CCC: $22.00
Published on Web 03/09/2002

as the only *uniquely* applicable criterion of aromaticity/antiaromaticity,[16] Katritzky, et al.[17] and Jug[18] have argued that aromaticity is at least two-dimensional. Thus an effective examination of aromaticity/antiaromaticity should consider as many measures of aromaticity as possible.

The instability predicted for antiaromatic species has prevented the characterization of a sufficient number of species to allow an understanding of antiaromaticity to be developed. We have discovered that dications of fluorenylidenes **1**−**3**, formed by oxidation of their olefin

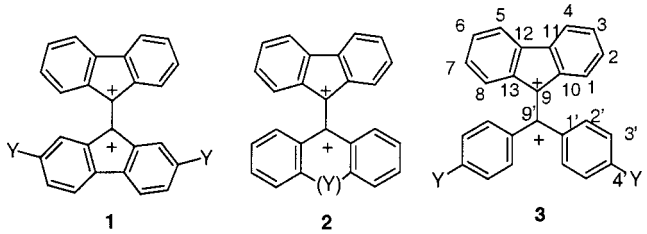

precursors with SbF_5 in SO_2ClF, possess appreciable antiaromaticity,[19−22] as evidenced by the substantial paratropic ^{1}H NMR shift of the fluorenyl ring. Calculation of magnetic susceptibility exaltation[12,15] and of nucleus independent shifts for **1a** and 9-substituted fluorenyl monocations confirmed the antiaromaticity of the fluorenylidene dications,[23] in contrast to the lack of antiaromaticity of the fluorenyl monocation.[24−26] We were anxious to identify a second experimental probe of antiaromaticity. Redox potential appeared to be a reasonable method because the stability of the dication, as suggested by the magnitude of the redox potential for oxidation, would be inversely correlated to the degree of antiaromaticity. In addition, one of the limitations of chemical oxidation with SbF_5, complexation of the Sb cation with substituents such as methoxy or bromo,[21,22] would not exist in the electrochemical oxidation, allowing the extension of studies to include these substituents and the subsequent examination of a linear free energy relationship. We report here our examination of the electrochemical oxidation to give dications of *p*-substituted diphenylmethylidene fluorenes and discuss their antiaromaticity, as evaluated through calculation of NICS and HOMA and the relationship between stability (redox potential) and antiaromaticity.

The Relationship between Experimental and Calculated Chemical Shift. There are several measures of ring current that are available through calculation, including nucleus independent chemical shift and magnetic susceptibility, which was used to calculate magnetic susceptibility exaltation. The nucleus independent chemical shift (NICS)[15] is based on the observation that protons in the center of an aromatic ring system experience a dramatic upfield shift because of the effect of the ring current.[27,28] By computing absolute magnetic shieldings at ring centers, effectively putting a dummy atom in the center of the ring system to "sense" the effect of the ring current, one can evaluate both the aromatic or antiaromatic character through the sign of the shielding, with aromatic species possessing negative NICS, as well as its relative magnitude through the size of the shielding. Because the local contributions of the σ bonds[29,30] might affect the magnetic shieldings, NICS values are normally calculated in the plane of the ring and at a distance, usually 1 Å, above the plane of the ring. Magnetic susceptibility exaltation refers to an absolute susceptibility that is larger than that expected on the basis of an incremental system.[11] NICS is usually calculated with the GIAO method in the Gaussian suite of programs,[31,32] while magnetic susceptibility is most commonly calculated using the IGLO program.[33]

The absolute value of either NICS or magnetic susceptibility is dependent upon the basis set used for the calculation[23] and it seemed prudent to begin with a comparison of the experimental NMR shifts for those dications for which measurements exist and their calculated shifts. The only dications in this group for which experimental data has been reported are **3c, 3e**, and **3f**.[22] The ^{13}C shifts were calculated with four different methods

(16) Schleyer, P. v. R.; Jiao, H. *Pure Appl. Chem.* **1996**, *68*, 209−218.
(17) Katritzky, A. R.; Karelson, M.; Sild, S.; Krygowski, T. M.; Jug, K. *J. Org. Chem.* **1998**, *63*, 5228−5231.
(18) Jug, K.; Koster, A. M. *J. Phys. Org. Chem.* **1991**, *4*, 163−9.
(19) Malandra, J. L.; Mills, N. S.; Kadlecek, D. E.; Lowery, J. A. *J. Am. Chem. Soc.* **1994**, *116*, 11622−11624.
(20) Mills, N. S.; Malandra, J. L.; Burns, E. E.; Green, A.; Unruh, K. E.; Kadlecek, D. E.; Lowery, J. A. *J. Org. Chem.* **1997**, *62*, 9318−9322.
(21) Mills, N. S.; Burns, E. B.; Hodges, J.; Gibbs, J.; Esparza, E.; Malandra, J. L.; Koch, J. *J. Org. Chem.* **1998**, *63*, 3017−3022.
(22) Mills, N. S.; Malinky, T.; Malandra, J. L.; Burns, E. E.; Crossno, P. *J. Org. Chem.* **1999**, *64*, 511−517.
(23) Mills, N. S. *J. Am. Chem. Soc.* **1999**, *121*, 11690−11696.
(24) Amyes, T. L.; Richard, J. P.; Novak, M. *J. Am. Chem. Soc.* **1992**, *114*, 8032−8041.
(25) Jiao, H.; Schleyer, P. v. R.; Mo, Y.; McAllister, M. A.; Tidwell, T. T. *J. Am. Chem. Soc.* **1997**, *119*, 7075−7083.
(26) See the following references for studies that support some degree of antiaromaticity for the fluorenyl monocation: Deno, N.; Jaruzelski, J.; Schriesheim, A. *J. Am. Chem. Soc.* **1955**, *77*, 3044−3051; Breslow, R.; Chang, H. W. *J. Am. Chem. Soc.* **1961**, *83*, 3727−3728; Allen, A. D.; Colomvakos, J. D.; Oswald, S. T.; Tidwell, T. T. *J. Org. Chem.* **1994**, *59*, 7185−7187.
(27) Mitchell, R. H. *Chem. Rev.* **2001**, *101*, 1301−1316.
(28) Gomes, J. A. N. F.; Mallion, R. B. *Chem. Rev.* **2001**, *101*, 1349−1384.
(29) Fleischer, U.; Kutzelnigg, W.; Lazzeretti, P.; Mühlenkamp, V. J. *J. Am. Chem. Soc.* **1994**, *116*, 5298−306.
(30) Schleyer, P. v. R.; Jiao, H.; van Eikema Hommes, N. J. R.; Malkin, V. G.; Malkina, O. L. *J. Am. Chem. Soc.* **1997**, *119*, 12669−12670.
(31) Frisch, M. J.; Trucks, G. W.; Schlegel, H. B.; Scuseria, G. E.; Robb, M. A.; Cheeseman, J. R.; Zakrzewski, V. G.; Montgomery, J., J. A.; Stratmann, R. E.; Burant; Dapprich, S.; Millam, J. M.; Daniels, A. D.; Kudin, K. N.; Strain, M. C.; Farkas, O.; Tomasi, J.; Barone, V.; Cossi, M.; Cammi, R.; Mennucci, B.; Pomelli, C.; Adamo, C.; Clifford, S.; Ochterski, J.; Petersson, G. A.; Ayala, P. Y.; Cui, Q.; Morokuma, K.; Malick, D. K.; Rabuck, A. D.; Raghavachari, K.; Foresman, J. B.; Cioslowski, J.; Ortiz, J. V.; Baboul, A. G.; Stefanov, B. B.; Liu, G.; Liashenko, A.; Piskorz, P.; Komaromi, I.; Gomperts, R.; Martin, R. L.; Fox, D. J.; Keith, T.; Al-Laham, M. A.; Peng, C. Y.; Nanayakkara, A.; Gonzalez, C.; Challacombe, M.; Gill, P. M. W.; Johnson, B.; Chen, W.; Wong, M. W.; Andres, J. L.; Gonzalez, C.; Head-Gordon, M.; Replogle, E. S.; Pople, J. A. *Gaussian 94*, A.7 ed.; Gaussian, Inc.: Pittsburgh, PA, 1998.
(32) Frisch, M. J.; Trucks, G. W.; Schlegel, H. B.; Gill, P. M. W.; Johnson, B. G.; Robb, M. A.; Cheesman, J. R.; Keith, T.; Petersson, G. A.; Montgomery, J. A.; Raghavachari, K.; Al-Laham, M. A.; Zakrzewski, V. G.; Ortiz, J. V.; Foresman, J. B.; Cioslowski, J.; Stefanov, B. B.; Nanayakkara, A.; Challacombe, M.; Peng, C. Y.; Ayala, P. Y.; Chen, W.; Wong, M. W.; Andres, J. L.; Replogle, E. S.; Gomperts, R.; Martin, R. L.; Fox, D. J.; Binkley, J. S.; Defrees, D. J.; Baker, J.; Stewart, J. P.; Head-Gordon, M.; Gonzalez, C.; Pople, J. A. *Gaussian 98*, Version E.2 ed.; Gaussian, Inc.: Pittsburgh, PA, 1995.
(33) Kutzelnigg, W.; Schindler, M.; Fleischer, U. *NMR, Basic Principles and Progress*; Springer-Verlag: Berlin, Germany, 1990.

Table 1. Experimental[a] and Calculated[b] ^{13}C NMR Shifts for Dications 3c ,3e, and 3f

	3c		3e		3f	
	exptl	B3LYP/ 6-31G(d)	exptl	B3LYP/ 6-31G(d)	exptl	B3LYP/ 6-31G(d)
1,8	146.6	133.92	147.1	133.98	146.2	133.75
2,7	136.1	125.28	136.6	125.51	134.2	124.90
3,6	159.4	150.41	160	150.92	158.4	149.75
4,5	130.9	121.00	131.4	121.18	130.1	120.40
9	198.4	190.26	198.5	189.68	201.2	192.63
10,13	149.8	138.54	149.8	138.59	148.8	138.49
11,12	152.2	141.79	152.6	141.85	151.8	141.63
9′	182.4	162.72	176	142.28	180.3	165.29
1′	135.1	122.74	133.8	120.61	134.2	122.44
2′	133.6	125.26	147.1	135.48	141.4	125.30
6′	133.6	130.21	147.1	130.25	141.4	132.53
3′	133.6	122.97	122.2	112.91	133	122.91
5′	133.6	124.04	122.2	112.10	133	124.26
4′	163.4	165.51	181.3	168.45	169.1	162.66

[a] Mills, N. S.; Malinky, T.; Malandra, J. L.; Burns, E. E.; Crossno, P. *J. Org. Chem.* **1999**, *64*, 511−517. [b] Geometries optimized at B3LYP/6-31G(d); chemical shift calculations using GIAO method.

and/or basis sets, GIAO at the RHF level with basis set 6−312G(d), with the density functional theory method using the B3LYP functionals with the 6−312G(d) basis set, and from the IGLO[33] method with basis sets DZ and II; see the Supporting Information. As expected, all methods show a linear relationship between experimental and calculated shifts, but the quality of that correlation varies with the method, with the best correlation for the density functional theory method, with a range of r from 0.967 to 0.998. In addition, the absolute magnitude of the ^{13}C shifts calculated using B3LYP/6-31G(d) were closer to the experimental values, as shown in Table 1. The ratio of experimental to calculated shifts for all carbons was 1.08 ppm, with a standard deviation of 0.03. A good correlation between experimental ^{13}C NMR shifts and shifts calculated with density functional theory for aliphatic cations has been reported recently.[34] Interestingly, Vrcek et al.[34] found that in their systems calculations overestimated the magnitude of the shifts, with a ratio of $\delta_{exp}/\delta_{calc}$ of 0.95−0.98, depending on the carbon considered.

The agreement between the experimental and calculated proton shifts for **3c, 3e**, and **3f**[22] is not quite as good; see the Supporting Information. The correlations for shifts calculated by the IGLO method are particularly poor. The GIAO method gives $r = 0.915$ for the correlation of all proton shifts using restricted Hartree−Fock basis sets and $r = 0.936$ for calculation using density functional theory methods. The correlation improves when only the protons of the fluorenyl systems are considered: $r = 0.930$ for RHF calculations and 0.952 for density functional theory calculations. The proton shifts calculated with density functional theory methods, shown in Table 2, were also closest to the experimental values, with the ratio of $\delta_{exp}/\delta_{calc}$ of 0.90 for all protons, except those of the methyl substituent and 0.89 for fluorenyl protons only.

While the correlation of calculated carbon shifts with experimental shifts is good for all methods, the relatively poor quality of the correlation for proton shifts calculated by the IGLO method with these basis sets calls into question the quality of other magnetic properties such as magnetic susceptibility and magnetic susceptibility exaltation. Proton shifts are much more sensitive than carbon shifts to those properties such as the presence of a ring current, which are characteristic of aromatic/antiaromatic systems. Thus, we have chosen to use only magnetic properties calculated by the GIAO method, such as nucleus independent chemical shift (NICS), as the measure of antiaromaticity, rather than magnetic susceptibility exaltation calculated by the IGLO method using the DZ or II basis set.

Table 2. Experimental[a] and Calculated[b] ^{1}H NMR Shifts for 3c, e, and f

	3c		3e		3f	
	exptl	B3LYP/ 6-31G(d)	exptl	B3LYP/ 6-31G(d)	exptl	B3LYP/ 6-31G(d)
H-1	4.58	4.99	4.44	5.06	4.80	5.08
H-2	4.89	5.59	4.75	5.65	5.06	5.64
H-3	5.69	6.50	5.54	6.53	5.86	6.53
H-4	4.98	5.61	4.83	5.64	5.12	5.68
H-2′	7.2	8.14	7.2	7.22	7.1	8.11
H-6′	7.2	6.93	7.2	8.49	7.1	7.06
H-3′	6.84	7.70	6.43	7.38	6.78	7.71
H-5′	6.84	7.70	6.43	7.53	6.78	7.57

[a] Mills, N. S.; Malinky, T.; Malandra, J. L.; Burns, E. E.; Crossno, P. *J. Org. Chem.* **1999**, *64*, 511−517. [b] Geometries optimized at B3LYP/6-31G(d); chemical shift calculations using GIAO method.

Table 3. Nucleus Independent Shift Calculations (NICS)[a,b] for 3a−g

compd	NICS-5	NICS-6
3a	33.1 (24.0)	16.2 (10.0)
3b	31.6 (22.6)	14.5 (8.6)
3c	31.9 (22.9)	14.8 (8.9)
3d	32.6 (23.1)	15.5 (8.9)
3e	32.2 (22.6)	14.9 (9.1)
3f	31.3 (22.2)	13.8 (7.9)
3g	30.1 (21.2)	12.5 (7.0)
1, Y=H	30.1 (21.4)	14.3 (8.4)
fluorenyl cation	29.0 (19.6)	9.85 (4.7)

[a] Calculated with GIAO at B3LYP/6-31G(d)//B3LYP/6-31G(d). [b] The value in parentheses is for NICS 1 Å above ring.

Nucleus Independent Chemical Shift Calculations; Use of Magnetic Criteria To Evaluate Antiaromaticity. The NICS values were calculated using density functional theory for **3a**−**g** and are listed in Table 3. The NICS values are calculated for the five- and six-membered rings for ghost atoms centered in the plane of the ring and at a distance 1 Å above the plane. For comparison, the NICS values for **1**, Y=H, and the fluorenyl cation are included in the table. It is apparent that the NICS values for **3** are much more like those of **1** than those of the fluorenyl cation, suggesting at the very least a ring current in **3** and **1** that is more paramagnetic than that found in the fluorenyl cation. For **3c, 3e**, and **3f**, the ring current results in an average chemical shift, δ_{ave}, for the protons of the fluorenyl system of 5.04, 4.89, and 5.21 ppm, respectively, compared with δ_{ave} of the 9-substituted fluorenyl cation of 7.33−7.75 ppm.[35]

The effect of the substituents on the antiaromaticity of **3**, as evaluated through NICS calculations, can be assessed by the use of substituent coefficients in a linear

(34) Vrcek, V.; Kronja, O.; Siehl, H.-U. *J. Chem. Soc., Perkin 2* **1999**, 1317−1321.

(35) Olah, G. A.; Prakash, G. K. S.; Liang, G.; Westerman, P. W.; Kunde, K.; Chandrasekhar, J.; Schleyer, P. v. R. *J. Am. Chem. Soc.* **1980**, *102*, 4485−4492.

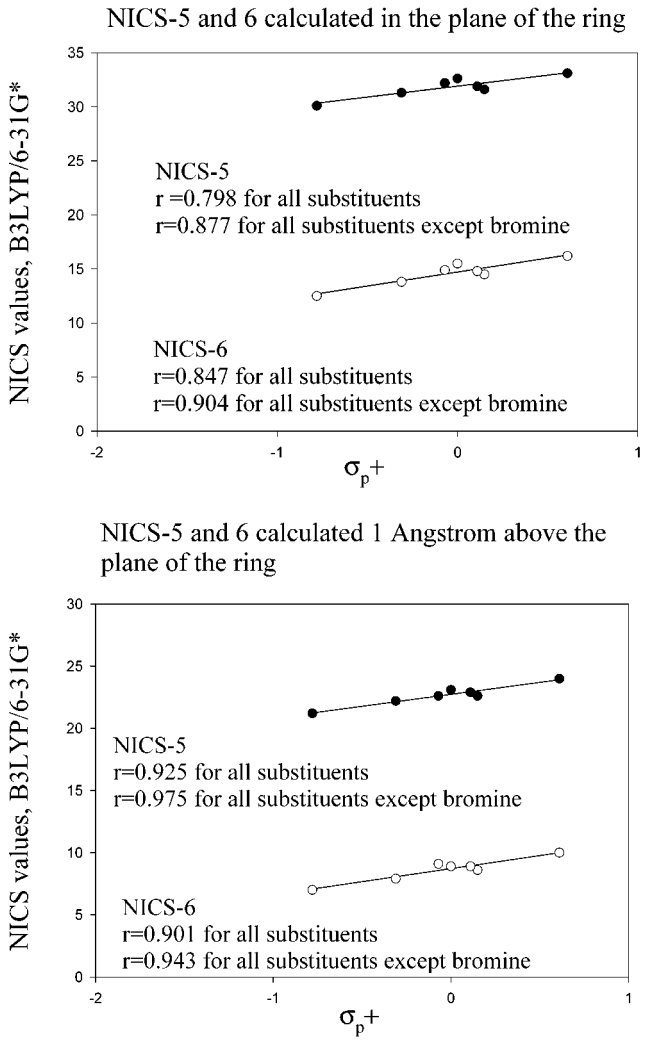

Figure 1. NICS values vs σ_p^+.

free energy relationship. The best correlation with the NICS values is with the σ_p^+ coefficients from Brown and Okamoto.[36,37] As can be seen from Figure 1, there is a good correlation with NICS values in the plane of the ring, which improves very slightly for the NICS-5 values 1 Å above the ring, suggesting that there are some local contributions to the magnetic shift. We also considered the correlation without the inclusion of values for the brominated derivative, **3b**, and the correlation is slightly better, as indicated in the figure. Because calculations with large atoms such as bromine benefit from larger basis sets, it is not unexpected that the NICS values for this compound are not as accurate.

Larger, more positive values for NICS indicate a greater degree of antiaromaticity; thus, electron-withdrawing substituents, with more positive values of σ_p^+, force upon these dications a greater degree of antiaromaticity.

Electrochemical Oxidation of Diphenylmethylidene Fluorenes; Use of Redox Potentials as Energetic Criteria in the Evaluation of Antiaromaticity. The oxidation of the olefin precursors to **3a**−**g** and **4a**−**g** were examined by cyclic voltametry in deaerated

Table 4. Electrochemical Oxidation to Cation Radical and Dication of Substituted Diphenylmethylidenefluorenes 4a−g[a,b]

Y	$E_{1/2}$, cation radical	i_{pa}/i_{pc}[c]	ΔE_p (mV)	$E_{1/2}$, dication	i_{pa}/i_{pc}[c]	ΔE_p (mV)
CF_3, **4a**	1.39	*d*	160	1.63*e*	*d*	150*e*
Br, **4b**	1.21	1.1	120	1.45	1.0	120
Cl, **4c**	1.20	1.2	120	1.42	0.9	140
H, **4d**	1.13	1.1	130	1.46	1.0	180
F, **4e**	1.14	1.1	130	1.41	0.9	120
CH_3, **4f**	1.00	1.1	120	1.33	1.2	140
OCH_3, **4g**	0.81	0.9	120	1.15	0.8	140

[a] Potentials in V vs a Ag/Ag^+ reference electrode. [b] Scan rate = 50 V/s. [c] i_{pa} =peak anodic current; i_{pc}=peak cathodic current. [d] Because of the poorly resolved voltamograms (see Figure 2), it was impossible to evaluate the ratio of currents. [e] Data for scan rate at 102 V/s; see the text.

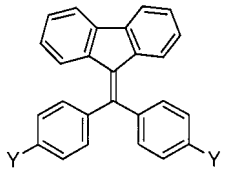

4

a, Y=CF_3
b, Y=Br
c, Y=Cl
d, Y=H
e, Y=F
f. Y=CH_3
g. Y=OCH_3

CH_2Cl_2 containing 0.2 M solution of tetrabutylammonium tetrafluoroborate (TBAF). The solvent with supporting electrolyte was dried by passing it through a column of dried alumina just prior to use. Oxidation with a 1.6 mm diameter electrode gave irreversible oxidation to the dication at all scan rates accessible, presumably due to its reaction with the traces of residual water in the solution. When the electrode was changed to a 10 μm diameter microelectrode, allowing an increase in scan rates to 25−102 V/s, the cyclic voltamograms showed reversible behavior. Reversibility in the oxidation to both cation radical and dication of **4b**−**g** was indicated by the ratio of peak currents (Table 4) and by the invariance of E_{pa} and E_{pc} with scan rates from 25 to 102 mV.[38] The cyclic voltamograms of **4a** at scan rates from 25 to 102 V/s did not give well-resolved peaks at scan rates less than 102 V/s, so determination of the redox potential for oxidation was made at 102 V/s. However, the plot of voltamograms at scan rates from 25 to 102 V/s (Figure 2) shows invariance of the E_{pa} and E_{pc} with scan rate and suggests that this too is a reversible oxidation. Figure 2 also includes a plot of scan rates for the oxidation of **4e** that is more representative of the typical cyclic voltamograms for this system.

To determine the effect of the substituent on the redox potential for oxidation for formation of cation radical and dication, a plot was made of the redox potential for oxidation ($E_{1/2}$) of each vs a substituent coefficient, σ. The best correlation was with σ_p^+,[36,37] which gave a correlation coefficient (r) of 0.997 for formation of the cation radical and 0.972 for formation of the dication. The slope of the

(36) Brown, H. C.; Okamoto, Y. *J. Am. Chem. Soc.* **1958**, *80*, 4979−87.

(37) Hansch, C.; Leo, A.; Taft, R. W. *Chem. Rev.* **1991**, *91*, 165−195.

(38) See Supporting Information for cyclic voltamograms of **4a**−**g** and a table of redox potentials as a function of scan rate for **4a**−**g**.

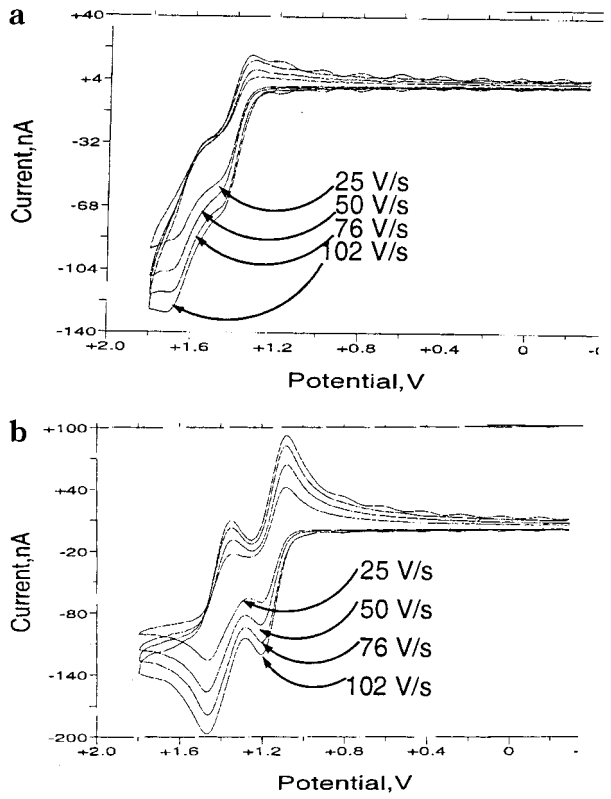

Figure 2. Voltamograms vs scan rate for **4a** and **4e**.

line for cation radical formation was about a third greater than that for formation of the dication, indicating the greater effect of the substituent on cation radical formation than on formation of the dication. The most electron-withdrawing substituents had the largest redox potentials for formation of the cation radical and dication by oxidation; thus, the electron-withdrawing substituents gave the least stable cation radicals and dications.

The nature of the cation radical remains to be determined, that is, whether the positive charge is localized in the fluorenyl system or on the diphenylmethyl carbon. The greater interaction between the substituent and the redox potential for oxidation for formation of the cation radical than for the formation of the dication suggests that the positive charge is located primarily in the diphenylmethyl group, with the radical localized in the fluorenyl group. This is consistent with the findings of Luisa et al., who examined the oxidation of **4c**−**g**.[39]

For redox potentials to be used as a measure of stability to assess antiaromaticity, they must be compared with the redox potentials for a model system that could not possess antiaromaticity. We chose to examine the oxidation of a series of *p*-substituted tetraphenylethylenes, **5**. Electrochemical oxidation of tetraphenylethylene or *p*-substituted tetraphenylethylenes substituted with electron-donating substituents have been shown to fall in one of three categories: (a) two well-separated one-electron processes; (b) two poorly separated, unresolved, one-electron processes; or (c) direct two-electron processes, or at least two one-electron processes in which the second occurs more readily than the first, depending on the solvent and the compound.[40] Examination of the oxidation of **5**, substituted with electron-withdrawing

Table 5. Electrochemical Oxidation to Cation Radical and Dication of Substituted Tetraphenylethylenes 5a−g[a,b]

Y	$E_{1/2}$, cation radical	i_{pa}/i_{pc}[c]	ΔE_p (mV)	$E_{1/2}$, dication	i_{pa}/i_{pc}[c]	ΔE_p (mV)	ΔE for the first and second oxidations, mV
CF_3, **5a**	1.59	*d*	160	1.84	*d*	20	190
Br, **5b**	1.22	1.3	110	1.35	1.8	110	130
Cl, **5c**	1.20	1.8	120	1.36	0.9	140	140
H, **5d**	1.06	1.4	120	1.33	1.6	160	290
F, **5e**	1.10	1.0	130	1.24	0.8	120	140
CH_3, **5f**	0.80	1.2	120	1.06	0.8	110	250
							270[e]
OCH_3, **5g**	0.58[f]	0.93[f]	190[f]				130
							120[e]

[a] Potentials in V vs a Ag/Ag^+ reference electrode, which was calibrated vs ferrocene, $E_{1/2}$ = 0.13 V. [b] Scan rate = 50 V/s. [c] i_{pa} =peak anodic current; i_{pc}=peak cathodic current. [d] i_{pc} was difficult to determine from the return scan. [e] Reference 46. [f] Because of the poorly resolved voltamogram, the $E_{1/2}$, difference in peak potentials, and ratio of currents were determined for the oxidation and reduction processes combined, rather than for each individual step.

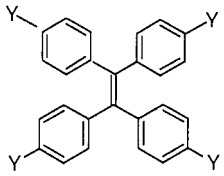

5

a, Y=CF_3
b, Y=Br
c, Y=Cl
d, Y=H
e, Y=F
f. Y=CH_3
g. Y=OCH_3

groups, showed no oxidation waves in the THF redox window.[41] The electrochemistry is further complicated by the ability of the cation radical of tetraphenylethylene to disproportionate to dication and neutral ethylene.[42] Furthermore, the oxidation of tetraphenylethylene to the dication by electrochemical[43,44] or chemical[45] methods results in cyclization to 9,10-diphenylphenanthrene. By using (ultra)microelectrodes and fast scan rates, we have been able to observe two waves for oxidation of **5** to cation radical and then to dication. The redox potentials, ΔE, and i_{pa}/i_{pc} are reported in Table 5. The values for **5f** and **5g** are consistent with those from recent literature.[46] The cyclic voltamograms for **5d**−**g** appear to be reversible, based on the invariance with peak potential as a function of scan rate[47] and the ratio of peak currents. The redox behavior of **5b** and **5c** also appears to be reversible, based on the invariance with peak potential as a function of scan rate. The ratio of peak currents was less supportive

(39) Luisa, M.; Franco, M. B.; Herold, B. J. *J. Chem. Soc., Perkin Trans. 2* **1988**, 443−449.

(40) Phelps, J.; Bard, A. J. *J. Electroanal. Chem.* **1976**, *68*, 313−335.

(41) Muzyka, J. L.; Fox, M. A. *J. Org. Chem.* **1991**, *56*, 4549−4552.

(42) Steckhan, E. *Electrochim. Acta* **1977**, *22*, 395−99.

(43) Aalstad, B.; Ronlan, A.; Parker, V. D. *Acta Chem. Scand. B* **1982**, *36*, 199−202.

(44) Stuart, J.; Ohnesorge, W. E. *J. Am. Chem. Soc.* **1971**, *93*, 4531−6.

(45) Olah, G. A.; Grant, J. L.; Spear, R. J.; Bollinger, J. M.; Serianz, A.; Sipos, G. *J. Am. Chem. Soc.* **1976**, *98*, 2501−2507.

(46) Rathore, R.; Lindeman, S. V.; Kumar, A. S.; Kochi, J. S. *J. Am. Chem. Soc.* **1998**, *120*, 6931−6939.

(47) See Supporting Information for cyclic voltamograms of **5a**−**g** as a function of scan rate.

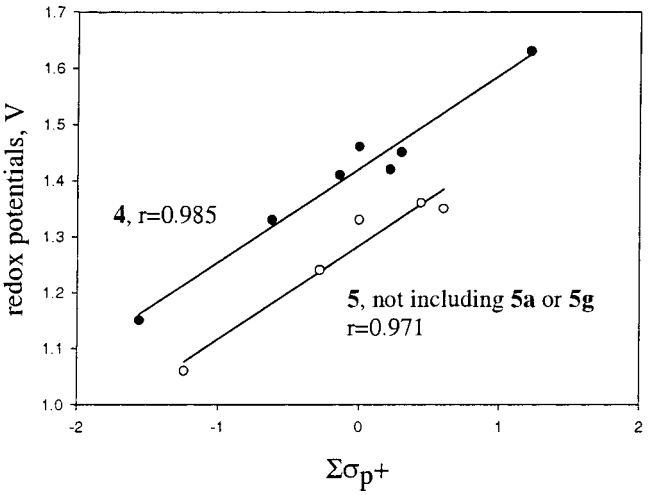

Figure 3. Redox potentials for formation of dications of **4** and **5** vs $\Sigma\sigma_p^+$.

of reversibility, but the difficulty of assessing the baseline on the reverse scan made determination of the cathodic current difficult for **5b** and **5c**. Compound **5a** is at best quasireversible. The separation between oxidation potentials for **5** is in general smaller than that observed for **4**. In the limiting case, where there is no separation between oxidation potentials, the so-called "inverted potential",[48] the cause of the inversion of potentials is due to changes in structure upon oxidation. Kochi et al.[46] have quantified the structural changes upon oxidation of **5g** to cation radical and then dication and have observed a number of changes, including substantial changes in the torsional angle that represents the conformation of the anisyl group with respect to the ethylenic bond and in the angle that reflects rotation around the carbons of the (former) ethylenic bond. In our systems, there is much less conformational mobility for **4** than for **5**, because two of the phenyl rings are confined in the fluorenyl system.

Comparison of the potentials for formation of the dications of **5** with those for the dications of **4** shows that for all substituents except CF_3 the redox potentials for formation of the fluorenylidene dications are more positive than those for the formation of the tetraphenylethylene dications, suggesting that the fluorenylidene dications are less stable than the tetraphenylethylene dications. The comparison is not perfect, however, because of the increased conformational mobility in **5**, which can affect the redox potential, and because the tetraphenylethylene dications have two more substituents, allowing either greater stability or greater instability, depending on the electron-donating or -withdrawing abilities of the substituent. The differing effects of the substituents can be sorted out through examination of the relationship between the redox potentials for formation of the dications vs the sum of the σ^+ values (Figure 3). It is apparent that the redox potential for formation of the fluorenylidene dications is a bit larger than that for formation of the tetraphenylethylene dications, but the difference is not great.Characterization of **3** as antiaromatic based on magnetic properties would suggest enhanced instability for **3** in comparison with a reference system, and to the extent that $\mathbf{5}^{2+}$ is an appropriate reference system, this decrease in stability is not dramatic. It is difficult to find many examples of instability due to antiaromaticity where the instability is quantified through redox potentials. Breslow et al.[49] examined the redox behavior of a series of quinones, including **6** and **7**, and concluded that there was substantial antiaroma-

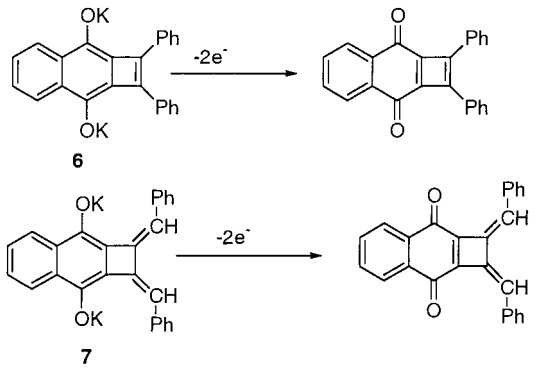

ticity in the cyclobutadiene ring of the oxidation product of **6**. However, the oxidation potentials for loss of two protons from **6** and **7** only differ by 200 mV, which is not that far removed from the differences between **4** and **5**, when correction for the additional substituents in **4** is made.

HOMA Values; Use of a Structural Measure of Antiaromaticity. Among the properties of potentially aromatic compounds that can be evaluated experimentally are the C−C bond lengths that in benzene are equal and intermediate in length between single and double bonds. Thus, an increase in bond length and a deviation from the optimal length found in benzene are considered as evidence of a decrease of aromaticity.[6] The harmonic oscillator model of aromaticity (HOMA)[7,8] examines the deviation of bond lengths from the optimal bond length found in benzene as shown below

$$\mathrm{HOMA} = 1 - \frac{\alpha}{n}\sum(R_{\mathrm{opt}} - R_{\mathrm{i}})^2$$

where n is the number of bonds taken in the summation and α is an empirical constant chosen to give HOMA = 0 for the hypothetical Kekulé structure of cyclohexatriene (where the bond lengths for C−C bonds are equal to the bond lengths in an acyclic polyene, 1,3-butadiene) and HOMA = 1 for the system in which the C−C bond lengths are all equal to the optimal length, i.e., benzene for hydrocarbon systems. The quantity R_{opt} is 1.388 Å for C−C bonds, R_{av} stands for the average bond length, and R_{i} is the individual bond length.

It is possible to separate the equation to reflect the effect of changes in the average bond length, which is presumed to be a term reflecting the energy cost of distortions from the optimal

$$\mathrm{HOMA} = 1 - \left[\alpha(R_{\mathrm{opt}} - R_{\mathrm{av}})^2 + \frac{\alpha}{n}\sum(R_{\mathrm{av}} - R_{\mathrm{i}})^2\right] = 1 - \mathrm{EN\text{-}GEO}$$

length and denoted EN, and to reflect the effect of increased bond length alternation, which is considered a term reflecting geometry, GEO, as shown below.

(48) Evans, D. H.; Hu, K. *J. Chem. Soc., Faraday Trans.* **1996**, *92*, 3983−3990.

(49) Breslow, R.; Murayama, D. R.; Murahashi, S.-I.; Grubbs, R. *J. Am. Chem. Soc.* **1973**, *95*, 6688−6699.

Table 6. HOMA Values for 3a−g, 1, and the Fluorenyl Cation[a]

				5-ring			6-ring		
	GEO	EN	HOMA	GEO	EN	HOMA	GEO	EN	HOMA
3a	0.18	0.18	0.64	0.10	0.76	0.14	0.10	0.08	0.82
3b	0.18	0.18	0.64	0.10	0.77	0.13	0.09	0.08	0.83
3c	0.18	0.18	0.64	0.10	0.77	0.14	0.10	0.08	0.82
3d	0.18	0.18	0.64	0.10	0.76	0.14	0.10	0.08	0.82
3e	0.18	0.18	0.64	0.10	0.76	0.14	0.10	0.08	0.82
3f	0.18	0.17	0.64	0.10	0.76	0.13	0.09	0.08	0.83
3g	0.18	0.18	0.64	0.10	0.78	0.13	0.09	0.07	0.84
fluorenyl cation	0.19	0.15	0.66	0.17	0.66	0.17	0.10	0.07	0.83
1, Y=H	0.18	0.18	0.64	0.10	0.76	0.14	0.10	0.08	0.83

[a] Geometries optimized using density functional theory, B3LYP/6-31G(d). All bond lengths and selected bond angles and dihedral angles can be found in the Supporting Information.

Although experimental data for the bond lengths of these dications are probably impossible to obtain, satisfactory agreement between experimental data and geometry optimizations at the density functional theory level (B3LYP/6-31G(d)) suggests that examination of these systems through their calculated geometries would be appropriate.[50−52]

The HOMA values for **3** are shown in Table 6. Because the substituent has a discernible effect on the magnetic properties of the fluorenyl system, in terms of paratropic shift of the protons of **3c, 3e**, and **3f** and the NICS values for all systems, and in terms of stability, as demonstrated by redox potentials, we anticipated that there would be an equally obvious effect on bond lengths. As is apparent from the calculated values of HOMA in Table 6, there is basically no effect of the substituent on the calculated bond length. It is important to put the HOMA values in context, that is, what is expected for the magnitude of HOMA for a system that is indisputably antiaromatic? Krygowski et al.[53] examined the antiaromaticity of a series of neutral and charged $4n\pi$ annulenes. The singlet state of C_4H_4 had a HOMA-index value of −3.99, with the major contribution to the value from the term describing bond length alternation (GEO). The singlet cyclopentadienyl cation had a HOMA-index value of −1.34, again with the primary contribution to the value arising from the term for bond length alternation. For all $4n\pi$ annulenes studied, the singlet state is mostly dearomatized due to the strong bond length alternation.

Benzannulation of the cyclopentadienyl cation to give the fluorenyl cation was predicted to effectively remove the antiaromaticity of the fluorenyl cation.[25] The HOMA index for the fluorenyl cation whose geometry was optimized at the B3LYP/6-31G(d) level is shown in Table 6, with the calculated bond lengths available in the Supporting Information. The HOMA index value of 0.66 indicates a substantially decreased antiaromaticity compared with the cyclopentadienyl cation. Jiao et al.[25] attributed the decrease in antiaromaticity to the "counterbalancing" of the antiaromatic five-membered ring by the two 6π electron six-membered rings. An analysis of the HOMA index values for the five- and six-membered rings supports this conclusion; see Table 6. In comparison to the parent cyclopentadienyl cation, the primary contribution to the antiaromaticity of the five-membered ring is due to the longer average bond length rather than the bond length alternation.

We recently reported[23] a comparison of the antiaromaticity of 9-substituted fluorenyl cations with that of **1**, Y=H. Calculation of NICS values for the five- and six-membered rings and of magnetic susceptibility exaltation indicated that **1** possessed substantial antiaromaticity, in comparison to the fluorenyl cation. This result was consistent with the magnitude of the paratropic shift of the protons of **1**. The HOMA values of **1** are listed in Table 6, along with those for the unsubstituted fluorenyl cation. The smaller magnitude of the HOMA of **1** in comparison with that of the fluorenyl cation indicates that it is more antiaromatic, but the difference between the two species is much closer than is suggested by NICS values, magnetic susceptibility exaltation, or paratropic shifts. Again, the five-membered ring of **1** is more antiaromatic than the six-membered ring, with this result due primarily to bond elongation in that ring rather than bond length alternation. The HOMA values for **3** are closer to those of **1** than to those of the fluorenyl cation, suggesting that their antiaromaticity is more like that of **1**.

The relative invariance of the calculated bond lengths in these substituted dications and the constancy of the HOMA values is disturbing when HOMA values are suggested as a measure of aromaticity/antiaromaticity. At the very least, the HOMA values appear to be very insensitive probes. A greater concern lies in the comparison of these values with those from other systems. For example, the HOMA value for these systems is larger than that calculated for one of the rings of chrysene, which has HOMA = 0.56.[54] This would suggest that this ring of chrysene is more antiaromatic than these dications, but the calculated NICS value is −8.7, indicating aromaticity.[55] The primary contribution to the lower HOMA value in the five-membered rings of **3** is due to bond elongation rather than bond alternation, as was true for the cyclopentadienyl cation. Benzannulation of the fluorenyl system has a marked affect on the ability of the system to alter its geometry in a manner that might be related to aromaticity/antiaromaticity. For this reason, we think that caution must be used in conclusions drawn about relative aromaticity/antiaromaticity in sys-

(50) Evdokimov, A. G.; Kalb, A. J.; Koetzle, T. F.; Klooster, W. T.; Martin, J. M. L. *J. Phys. Chem. A* **1999**, *103*, 744−753.

(51) Rasul, G.; Prakash, G. K. S.; Olah, G. A. *J. Org. Chem.* **2000**, *65*, 8786−8789.

(52) Nendel, M.; Houk, K. N.; Tolbert, L. M.; Vogel, E.; Jiao, H.; Schleyer, P. v. R. *J. Phys. Chem. A* **1998**, *102*, 7191−7198.

(53) Krygowski, T. M.; Cyranski, M. K. *Tetrahedron* **1999**, *55*, 11143−11148.

(54) Cyranski, M. K.; Krygowski, T. M. *Tetrahedron* **1998**, *54*, 14919−14924.

(55) The NICS values reported in this article are done with a basis set that is known to overestimate aromaticity, but the proton chemical shifts for chrysene, from 7.64 to 8.79 ppm, are certainly not paratropic enough to suggest antiaromaticity.

Table 7. Comparison of Calculated Dihedral Angles for Phenyl Substituents with fluorenyl ring system[a]

compd	dihedral angle	planarity of fluorenyl ring[b]	range of deviation from 0°
3a	118.22	0.57	0.01−1.15
3b	122.29	0.99	0.18−2.00
3c	120.94	0.82	0.15−1.64
3d	117.38	0.61	0.00−1.23
3e	118.65	0.69	0.09−1.77
3f	119.00	0.68	0.07−1.39
3g	123.27	1.02	0.22−2.29

[a] Geometry optimized using DFT; B3LYP/6-31G(d). [b] Average of the absolute value of deviation from 0°.

tems that are not similar in terms of the amount of benzannulation.

Although the focus of HOMA values is on the changes on bond lengths as a function of changing aromaticity/antiaromaticity, other structural features of these dications might affect the degree of paratropicity of their chemical shifts. Specifically, the interaction of the phenyl rings with the fluorenyl ring system might affect the shifts of the fluorenyl protons. The absence of experimental data forces us to rely on the calculated geometries, which, as stated before, have been shown in a number of systems to match experimental data very well. The dihedral angles of the phenyl rings with the fluorenyl systems are listed in Table 7. It is obvious that variation in the dihedral angles for **3a**−**g** is relatively small, so this does not play a major role in the differences in the paratropicity of the fluorenyl systems. The planarity of the fluorenyl ring system was also assessed by examining the differences in the calculated dihedral angles for the fluorenyl ring system from 0°. The rings have maintained their planarity, with the deviation from planarity in a particular dihedral angle being less than 2.29°.

Examination of Antiaromaticity Using Structural, Magnetic, and Energetic Measures. The interrelationship between the criteria used to evaluate aromaticity/antiaromaticity is currently under debate. Schleyer has stated that "linear relationships exist among the energetic, geometric, and magnetic criteria of aromaticity and that these relationships even extend to antiaromatic systems."[56] Katritzky et al.[17] have used principal component or factor analysis to demonstrate that "aromaticity is a multidimensional phenomenon and that one component may be more aromatic than another in one dimension or another." [57] Our intent was to explore the relationships between these three criteria, as measured through redox potentials, HOMA values, and NMR shifts and NICS. However, the HOMA values for **3a**−**g** are sufficiently insensitive to changes in the electronic character of these cations that they cannot be used in any sort of internal comparison with the other criteria examined. In addition, concerns about the appropriateness of using these values to make judgments about aromaticity/antiaromaticity prevents us from drawing any conclusions about the relative antiaromaticity of these dications from the use of this criterion.

As noted in a recent review article, "NMR is without doubt the most frequently used experimental tool to decide whether a molecule is aromatic."[27] Unfortunately, we can use NMR data to evaluate substituent effects through linear free energy relationships only for those systems in which no complexation occurred, **3c, 3e**, and **3f**.[22] However, the quality of the correlation of experimental chemical shifts of **3c, 3e**, and **3f** with the shifts calculated by the density functional theory method, B3LYP/6-31G(d), and the implicit quality of other magnetic properties such as NICS suggests that NICS values can be calculated accurately for **3a**−**g** and used to evaluate the antiaromaticity of these systems.

Redox potentials for formation of the dications of **4** were obtained as a measure of stability/instability. As such, they show relatively little destabilization for dications of **4** compared to dications of **5**, although the amount of destabilization is roughly comparable to that of a cyclobutadienyl quinone that was described as "clearly antiaromatic".[49] The redox potentials for oxidation of **4** show enough variation to be appropriate for comparison with the magnetic properties examined, in contrast with HOMA values. Certainly the redox potentials allow an evaluation of relative stability within the fluorenylidene system.

We have therefore examined the relationship between magnetic and energetic criteria by looking at the correlation between NICS and redox potential. Since both the NICS values and the redox potentials show good correlation with σ_p^+, it would not be unexpected that there would be a correlation between NICS and redox potentials. That correlation is shown in Figure 4 and it is apparent that, as was seen before, the correlation is, in general, slightly better with the NICS values calculated at 1 Å above the plane of the ring and slightly better when the point for the brominated derivative is excluded. The correlation between NICS and redox potential is quite good. NICS has been shown to give a good correlation with measures of energetic stability[15] for systems with only a single ring, for which NICS was representative of the entire system. In our systems, the redox potential reflects the stability of the entire system, while the individual NICS values reflect the existence of a ring current in a particular ring of the fluorenyl ring system.

The original research, on compounds **3c**, **3d**, and **3f**, suggested that the fluorenyl systems possessed substantial antiaromaticity on the basis of the paratropic shift of the fluorenyl protons. This work extends that conclusion to substituted diphenylmethylidene fluorene dications that have a greater range of electron-donating and -withdrawing abilities. This has allowed the observation of a linear relationship between a second measure of antiaromaticity, the nucleus independent chemical shift, and substituent coefficients, which suggests that electron-withdrawing substituents increase the antiaromaticity of the cationic fluorenyl system.

The use of redox potentials to assess antiaromaticity is less satisfactory, because it appears that the destabilization afforded through antiaromaticity results in relatively small changes in redox potential in these and other systems. However, the good correlation between magnetic properties, such as NICS, and energetic properties, such as redox potential, suggests that those properties may share a common origin, that is, antiaromaticity. Of the properties examined, magnetic properties, such as paratropic NMR shifts and NICS, appear to be the most sensitive probes of antiaromaticity. We are exploring the use of other measures to probe the antiaromaticity of fluorenylidene dications and to use their behavior to

(56) Schleyer, P. v. R.; Freeman, P. K.; Jiao, H.; Goldfuss, B. *Angew. Chem., Int. Ed. Engl.* **1995**, *34*, 7−340.

(57) Krygowski, T. M.; Cyranski, M. K.; Hafelinger, G.; Katritzky, A. R. *Tetrahedron* **2000**, *56*, 1783−1796.

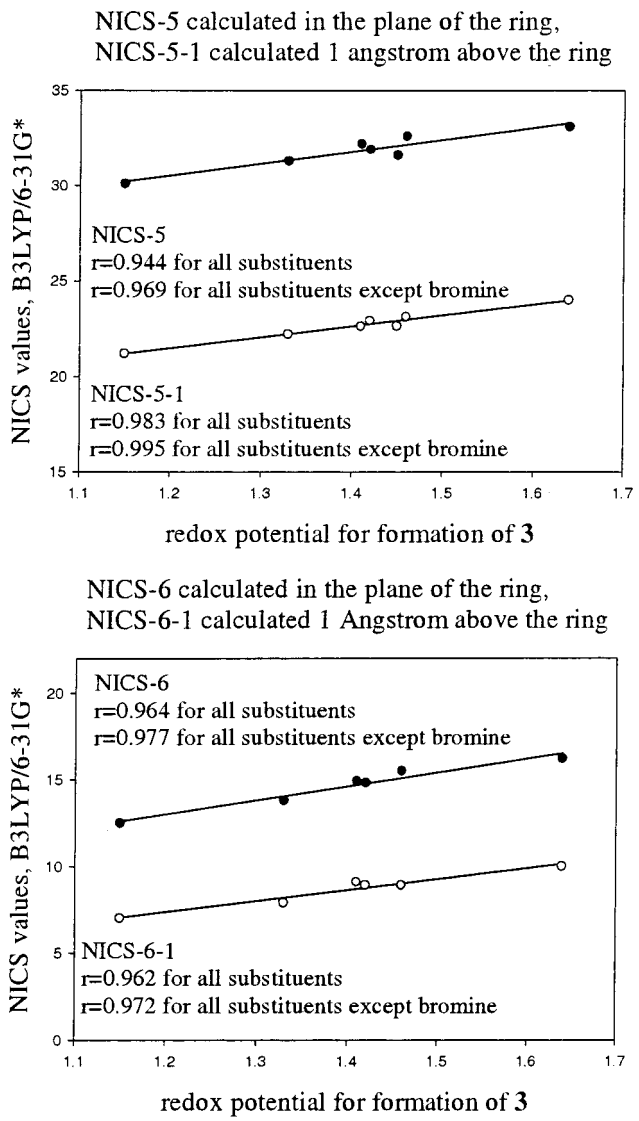

Figure 4. NICS-5 and NICS-6 vs redox potential for formation of **3.**

evaluate the multidimensional nature of aromaticity and antiaromaticity.

Experimental Section

Compounds **4a, b,** and **4g** were synthesized by Peterson olefination of the appropriate benzophenone with fluorene. Compounds **4c, 4e,** and **4f**[39] were synthesized by reaction of the fluorenyl anion with the appropriate benzophenone, followed by dehydration of the alcohol.[22] Compound **4d**[58] was synthesized according to the literature procedure. The benzophenones for **4b**−**g** were obtained from Aldrich Chemical Co. and were used without further purification. The benzophenone precursor for **4a** was synthesized from *p*-trifluoromethylbenzaldehyde via reaction with 4-trifluoromethylphenyllithium[59] followed by Swern oxidation to give the known ketone.[60] Tetraphenylethylene (Aldrich) was used as received, and *p*-substituted tetraphenylethylenes (**5**) were prepared by literature methods, usually by titanium-induced reductive coupling of the substituted benzophenones.[41]

Synthetic Procedures. Bis-(*p*-trifluoromethylphenyl)-methylidenefluorene (4a). To a solution of 9-trimethylsilylfluorene (0.76 g, 3.20 mmol) in 40 mL of THF at −78 °C was added *n*-butyllithium (1.40 mL of a 2.5 M solution in hexanes, 3.50 mmol). The resulting orange suspension was stirred at −78 °C for 10 min and then at 0 °C for 1.5 h. The reaction mixture was recooled to −78 °C and a solution of 4,4′-bis-trifluoromethylbenzophenone (1.11 g, 3.49 mmol) in 20 mL of THF was added via cannula. The cooling bath was removed and the orange solution was stirred for 12 h at room temperature. The reaction mixture was quenched with 50 mL of 10% aqueous HCl and extracted twice with 150 mL portions of diethyl ether. The organic layers were combined and washed successively with 150 mL each of 10% aqueous HCl, water, and saturated sodium chloride. The organic layer was separated and dried over magnesium sulfate, and the solvent was evaporated under reduced pressure. Recrystallization from hexane gave 1.06 g of bis-(*p*-trifluoromethylphenyl)methylidenefluorene as white plates (71% yield): mp 182−184 °C; ^{1}H NMR (400 MHz, $CDCl_3$) δ 7.70 (d, J = 8.0 Hz, 6 H), 7.50 (d, J = 8.0 Hz, 4 H), 7.28 (td, J = 7.6 Hz, J = 0.8 Hz, 2 H), 6.96 (td, J = 7.6 Hz, J = 1.2 Hz, 2 H), 6.57 (d, J = 8.0 Hz, 2 H); ^{13}C NMR (100 MHz, $CDCl_3$) δ 146.09, 141.19, 141.15, 138.03, 136.35, 130.74 (q, J_{CF} = 32.6 Hz), 130.35, 128.85, 127.05, 126.28 (q, J_{CF} = 3.8 Hz), 125.10, 124.25 (q, J_{CF} = 270.8 Hz), 119.82. Anal. Calcd for $C_{28}H_{16}F_6$: C, 72.10; H, 3.46; F, 24.44. Found: C, 72.00; H, 3.27; F, 24.63.

9-Bis-(4-bromophenyl)methylenefluorene (**4b**) was synthesized as above for **4a** to yield a yellow solid (62% yield): mp 206−208 °C; ^{1}H NMR (400 MHz, $CDCl_3$) δ 6.71 (d, J = 8.0 Hz, 2 H), 6.97 (td, J = 7.6 Hz, 1.2 Hz, 2 H), 7.22 (td, J = 8.4 Hz, J = 1.2 Hz, 4 H), 7.27 (td, J = 7.6 Hz, J = 1.2 Hz, 2 H), 7.55 (dd, J = 8.4 Hz, J = 1.8 Hz, 4 H), 7.69 (bd, J = 7.6 Hz, 2 H); ^{13}C NMR (100 MHz, $CDCl_3$) δ 119.67, 123.03, 125.02, 126.86, 128.37, 131.91, 132.39, 135.38, 138.44, 140.91, 141.60, 142.33. Anal. Calcd for $C_{26}H_{16}Br_2$: C, 63.96; H, 3.30; Br, 32.73. Found: C, 62.63; H, 3.31; Br, 31.26.

Electrochemistry. Cyclic voltammetric experiments were performed on a Bioanalytical Systems BAS-100B electrochemical analyzer. The electrode was a 10 μm platinum disk in glass, approximately 7 cm long and 0.3 cm in diameter, from Cypress Systems. The $Ag/AgNO_3$ reference electrode consisted of a silver wire in a saturated aqueous solution of $AgNO_3$. The counter electrode was 1 cm square platinum gauze.

Alumina was activated by flame drying under vacuum. A 0.2 M solution of tetrabutylammonium tetrafluoroborate (TBAF) in dried methylene chloride was passed through an alumina column directly into the electrolysis vessel, which had been dried in an oven at 130 °C. Argon was bubbled through the solution for 30 s and then a blanket of argon was maintained throughout voltammetric experiments. Alumina (ca. 1 g) and the desired compound (10 mg) were added, the electrodes were placed in the solution, and vigorous stirring was carried out magnetically for about 1 min to suspend the alumina.[61] Voltammetric measurements were made shortly after stirring was stopped, the solid phase being allowed to settle about 5 s. The working electrode was wiped with tissue before each measurement. Ferrocene was added to the solution after the measurements as an internal potential calibration. However, the potential required for oxidation to dication caused reaction with ferrocene in the methylene chloride solution, so it was only possible to verify the potential for formation of the cation radical by this method.

Computational Methods. Geometries were optimized at B3LYP/6-31G(d) density functional theory levels with the Gaussian 94 and 98 program packages.[31,32] The nucleus-independent chemical shifts (NICS [15]) in the ring centers were calculated at RHF/6-31G(d) and B3LYP/6-31G(d) using the GIAO approach with Gaussian 94 or 98. The magnetic susceptibilities were calculated with the IGLO [62,63] method and

(58) Hill, J. W.; Jenson, J. A.; Yaritz, J. G. *J. Chem. Educ.* **1986**, *63*, 916.
(59) Kelly, D. P.; Jenkins, M. J. *J. Org. Chem.* **1984**, *49*, 409−13.
(60) J., H. N.; Olah, G. A.; Prakash, G. K. S. *J. Am. Chem. Soc.* **1995**, *117*, 11205−10.
(61) Hammerich, O.; Parker, V. D. *Electrochim. Acta* **1973**, *18*, 519−522.
(62) Kutzelnigg, W.; Schindler, M.; Fleischer, U.; Springer-Verlag: Berlin, Germany, 1990.

basis sets DZ and II for all systems. The DZ basis set was constructed from the Huzinaga[64] (7s3p) set for carbon and the (3s/2s) set for hydrogen, contracting it to (4111/21) and augmenting it by a d-set for C ($\eta = 1.0$) and a p-set ($\eta = 0.65$) for H. Basis II was constructed from the Huzinaga[64] (9s5p) set for carbon and the (5s) set for hydrogen, contracting it to (51111/2111) and augmenting it by a d-set for C ($\eta = 1.0$) and a p-set ($\eta = 0.65$) for H.

Acknowledgment. We gratefully acknowledge the Welch Foundation (Grant 794) and the National Science Foundation (CHE-9820176, REU site) for their support of this work.

(63) Schindler, M.; Kutzelnigg, W. *J. Chem. Phys.* **1982**, *76*, 1919−1933.

(64) Huzinaga, S. *Approximate Atomic Wave Functions*; University of Alberta: Emondton, Alberta, Canada, 1971.

Supporting Information Available: ^{1}H and ^{13}C NMR spectra of **4a** and **4b**; cyclic voltamograms of **4a**−**g** and **5a**−**g**, including varying scan rates; a table of oxidation and reduction potentials as a function of scan rate for **4a**−**g**; cyclic voltamograms for **5a**-g, including those with varying scan rates; a table of calculated bond lengths, angles, and selected dihedral angles for **3a**−**g**; a table of calculated symmetries, total energies, and [*x*,*y*,*z*] coordinates; tables of experimental and calculated ^{13}C and ^{1}H NMR shifts for **3c**, **3e**, and **3f**. This material is available free of charge via the Internet at http://pubs.acs.org.

JO001776L